Double Resonance Spectroscopy in Rb Vapor Cell of Atomic Clock via Synthesizer

Ali Mirzaei, Danial Cheraghian, Mahnaz Asadolah Salmanpour, Mohammad Mosleh, and Seyedeh Mehri Hamidi*

Magneto-plasmoic Lab, Laser and Plasma Research institure, Shahid Beheshti University, Tehran, Iran.

Corresponding author email: m_hamidi@sbu.ac.ir

Received: Oct. 10, 2025, Revised: Mar. 07, 2026, Accepted: Mar. 11, 2026, Available Online: Mar. 13, 2026,
DOI: **Due to the current conditions, there is no possibility to buy DOI for papers. We hope to buy them as soon as possible.**

ABSTRACT— We aim to examine double resonance of Rb vapor cell via synthesizing the input 10 MHz frequency as standard atomic clock devices. For this purpose, we use the Voltage Controlled Oscillator onto the synthesizer and record double resonance between optical and microwave pumping. Our results show that the fabricated synthesizer, whose applied frequency is locked to a target frequency, can generate efficient coupling between these two main resonances in atomic media.

KEYWORDS: atomic media, Double resonance, magneto-plasmonic, Rb vapor.

I. INTRODUCTION

Double resonance spectroscopy is a powerful technique that enables precise measurement of hyperfine transitions in Rb atoms. By improving our understanding of hyperfine transitions and their behavior in the presence of magnetic fields, we can enhance the accuracy and reliability of time-measuring devices, which are vital for modern technology and scientific advancement.

Rubidium atoms (^{87}Rb) have a ground state that is split into two hyperfine energy levels due to the nonzero nuclear spin. The frequency corresponding to the transition between these levels lies within the microwave range. In this study, we employ the double-resonance spectroscopy method to investigate this transition [1],[2].

At present, the acquisition of double resonance spectra necessitates two distinct experimental configurations: one dedicated to optical resonance and the other to microwave resonance. The system must be capable of performing optical pumping while simultaneously applying a microwave field at the frequency corresponding to the atomic clock transition. In this setup, the microwave resonance is typically generated using a signal generator operating at approximately 6.834 GHz [3],[8].

The precision of time measurement by atomic clocks is one of the highest levels of accuracy ever achieved by humankind. These clocks utilize the physical properties of atoms to measure time, and they are capable of measuring time with accuracy down to the nanosecond or even better. In atomic clocks, time is measured based on the energy transitions within atoms. The extremely high accuracy of atomic clocks is due to the stability of the radio frequencies used to excite the atoms. Each atom, under identical conditions, consistently transfers its energy, and the frequency of this energy transition remains constant. This consistency in frequency allows atomic clocks to measure time with unparalleled precision. This extraordinary accuracy in time measurement has led to the widespread use of atomic clocks in applications such as Global Positioning System (GPS), satellite communications, physical research,

[Downloaded from mail.ijop.ir on 2026-11-26]

and the standardization of international time units.

When an external magnetic field is present, the hyperfine transition splits into several closely spaced components due to the Zeeman effect. Understanding these transitions is essential, as one of them remains unaffected by the applied magnetic field. This field-insensitive transition can serve as a frequency reference for time measurement, contributing to improved accuracy and stability of atomic clocks [11].

Double-resonance spectroscopy enables precise measurement of the transition rate between hyperfine levels, providing insight into the dynamics of Rb atoms and optimization of clock performance. Furthermore, by employing double-resonance spectroscopy, one can examine the effects of spin-exchange collisions on atomic spectra and determine the collision rate, thereby minimizing disturbances in the atomic clock and enhancing its precision.

A critical requirement for this device is the ability to maintain stable locking of both the frequency and the microwave power applied to the atomic ensemble. However, in the development of compact and cost-efficient atomic clocks, it is essential to minimize both the cost and physical footprint of the microwave field source [12],[13].

To address this, we employ a frequency synthesizer, which fulfills the same functional role in the microwave resonance setup namely, generating and stabilizing a microwave field at a well-defined frequency and power. Unlike the conventional signal generator, the synthesizer operates at a frequency of approximately 10 MHz, offering significant advantages in terms of compactness, power efficiency, and overall system integration [9],[11].

II. METHOD AND MATERIALS

The three-level model in microwave–optical double resonance (DR) is used for precise control of atomic states. This scheme involves two types of electromagnetic fields: a microwave field and an optical field, which together facilitate transitions among three specific energy levels.

We first examine the optical field, where optical pumping occurs. Optical pumping in warm rubidium vapor is a powerful technique in atomic physics. By precisely tuning the laser and understanding the interaction between light and atomic energy levels, this process has significant implications for the development of advanced technologies in timekeeping, magnetometry, and quantum information science. In rubidium atomic clocks, optical pumping is a crucial step for preparing rubidium atoms in a specific energy level to enable accurate frequency measurement.

In a Λ-type three-level system, as shown Fig. 1(a), there are two ground states and one excited state. One of the ground states interacts with the optical field, while the other does not. If there is a significant energy difference between the two ground states and the optical field frequency is resonant with the transition between one ground state and the excited state, the second ground state, which does not interact with the optical field, is naturally formed. In this experiment, a distributed feedback (DFB) laser with a wavelength of 795 nm was used for optical pumping. Precise wavelength adjustment was achieved by tuning the laser current and temperature. To reach optimal pumping conditions, both parameters were finely controlled so that the laser output frequency resonated with the $F_g = 2 \rightarrow F_e = 1$ transition of rubidium atoms.

The pumping light, whose frequency matches the $|5S_{1/2},\ F_g = 2\rangle \rightarrow |5P_{1/2},\ F_e = 1\rangle$ transition, excites atoms from the $|F=2\rangle$ ground state to the excited state. The excited atoms then return to the ground state, often to a different sublevel from where they started, due to the random nature of spontaneous emission. Repeated absorption and emission cycles lead to an accumulation of atomic population at the second ground level $|F=1\rangle$, resulting in a non-equilibrium distribution known as optical pumping.

[Downloaded from mail.ijop.ir on 2026-11-26]

Next, we consider the applied microwave field generated by the synthesizer. For double resonance to occur, a second field the microwave field is applied. If the applied frequency exactly matches the energy difference between the two ground levels, it can transfer atoms from the second level (which does not interact with light) to the upper ground level where optical pumping can take place. At this point, resonance occurs due to the microwave field, and double resonance is achieved through the combined action of the two fields. A key aspect of the microwave field is its frequency locking to the applied resonance frequency.

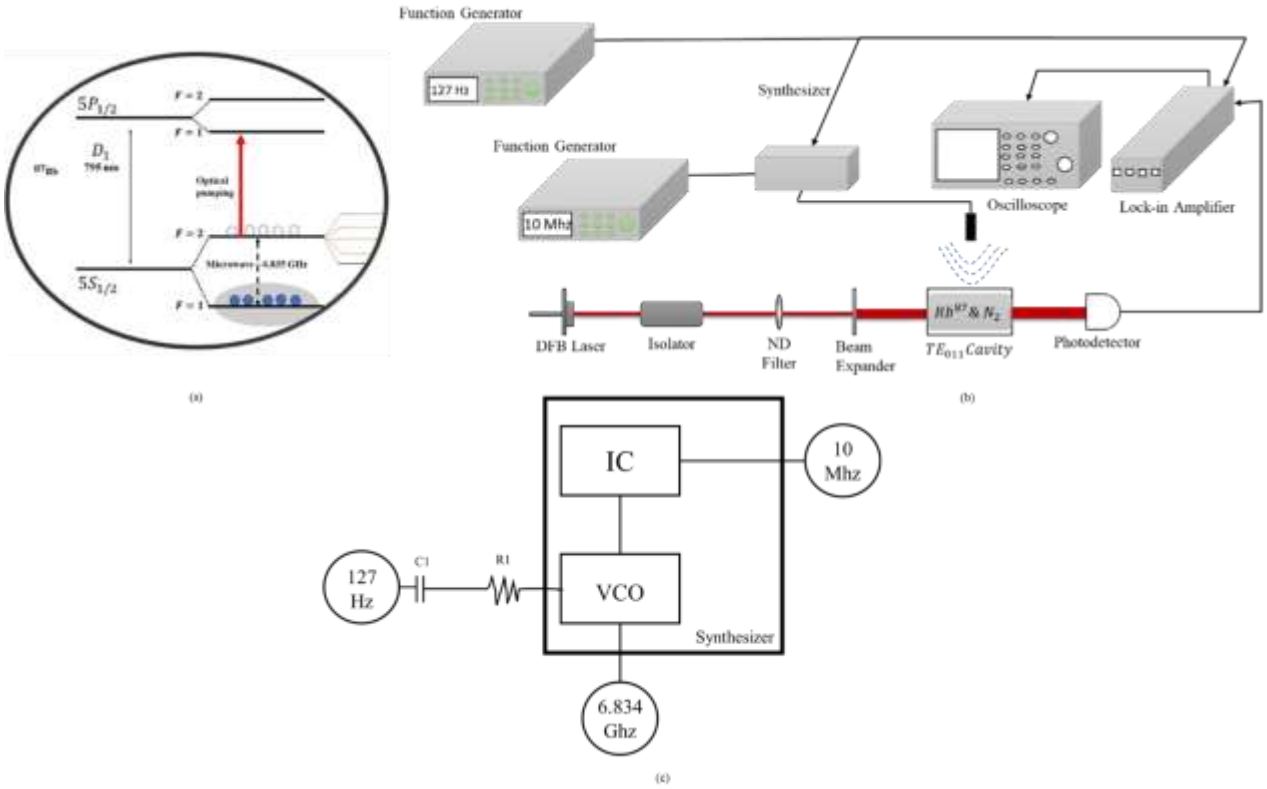


Fig. 1. (a) Fine and hyperfine structure of the Rb^{87} atom, illustrating the optical and microwave fields applied for double resonance. (b) Schematic diagram of the experimental setup used for the double resonance spectroscopy of Rb^{87} atoms, including the optical pumping configuration and the applied microwave field. (c) Block diagram of the frequency synthesizer, illustrating the main components responsible for generating, multiplying, and stabilizing the microwave output frequency.

Next, we consider the applied microwave field generated by the synthesizer. For double resonance to occur, a second field the microwave field is applied. If the applied frequency exactly matches the energy difference between the two ground levels, it can transfer atoms from the second level (which does not interact with light) to the upper ground level where optical pumping can take place. At this point, resonance occurs due to the microwave field, and double resonance is achieved through the combined action of the two fields. A key aspect of the microwave field is its frequency locking to the applied resonance frequency.

Two types of data acquisition were performed using a specific setup, where the main difference between these setups lies in the method of applying the microwave field to the vapor cell.

At the beginning, following a standard and routine procedure, the 795 nm DFB laser light passes through an optical isolator that prevents back reflections into the laser cavity. Next, the light intensity is adjusted using an ND filter, and then the beam is expanded by a beam expander to cover a larger active region of the cell, thereby exciting more atoms. In this setup, we used a cylindrical vapor cell containing

[Downloaded from mail.ijop.ir on 2026-11-26]

natural rubidium. During the optical pumping process, to ensure that only the rubidium-87 isotope is exciting, the laser current and temperature were tuned to match the desired transition.

A proportional-integral derivative (PID) controller circuit was employed to stabilize the cell temperature at 70°C. Additionally, a DC magnetic field was applied to compensate for the Earth's magnetic field, allowing us to focus solely on the 0-0 Zeeman transition. Under these conditions, the polarization of applied light becomes irrelevant to measurement.

Next, we focus on the key variable in this experimental setup: Here, the microwave field is applied using a signal generator. In these experiments, we initially apply a frequency of approximately 6.834 GHz. In order to obtain finer, sharper data with lower noise, we use the frequency modulation (FM) measurement method [10],[14].

In this experimental approach, to achieve frequency modulation, a 127 Hz signal with a voltage amplitude of 2.612 V is generated by a function generator and applied to the signal generator to modulate the microwave field.

The resulting microwave field, with a center frequency of 6.834 GHz and a power of 25 dBm, was then applied to the cell. After detection, the output signal was sent to a lock-in amplifier, where noise reduction and signal amplification were performed, improving the signal-to-noise ratio. Finally, the processed signal was transferred to the oscilloscope, and the data were recorded using a LabView-based data acquisition system (as shown in Fig. 2(a)).

In the second part of the data acquisition, a significant difference in the measurement setup is observed. In this section, the key device, the signal generator, was removed, and instead, a synthesizer was used to apply the microwave field. Here, rather than directly applying a frequency of 6.834 GHz, a 10 MHz input signal was applied to the synthesizer. Based on the internal coefficients and settings configured within the synthesizer, this input frequency was multiplied and converted to approximately 6.834 GHz.

In the synthesizer circuit, a frequency counter is connected to the input, responsible for regulating the overall operating frequency of the circuit. The internal configuration of the main IC determines the multiplication coefficients of the circuit's internal frequency-multiplier stages. Specifically, the input frequency is multiplied by a factor of 683.4 within the circuit and then compared with the output frequency of a crystal oscillator. In this experiment, the 10 MHz frequency served as the base or reference frequency.

To adjust the output frequency, the synthesizer was set to the (VTune) mode, which allows fine-tuning of the crystal oscillator output frequency. As shown Fig. 1(c), the main IC mentioned above compares the input and output frequencies, accounts for the internal scaling parameters, and ultimately stabilizes the oscillator's output frequency.

Because higher microwave power generally results in better signal quality, a power amplifier was added to the experimental setup after the synthesizer to amplify the microwave field. This is necessary since the microwave output power from the synthesizer is only 0 dBm. The amplifier increases the input power by approximately 25 dBm, ensuring sufficient field strength for data acquisition.

As shown Fig. 1(c) in the block diagram of the synthesizer, In the second part of the data acquisition (with synthesizer), after applying the 10 MHz frequency to the synthesizer, the output of the function generator is connected to the input capacitor C1, which is then linked to the resistor R1.

In this configuration, the resistor limits the current applied to the tuning pin of the oscillator inside the synthesizer, while the capacitor removes DC offset from the modulation signal. The modulation frequency, as previously mentioned, is 127 Hz, and a modulation voltage of 80 mV is applied to the capacitor by the function generator.

[Downloaded from mail.ijop.ir on 2026-11-26]

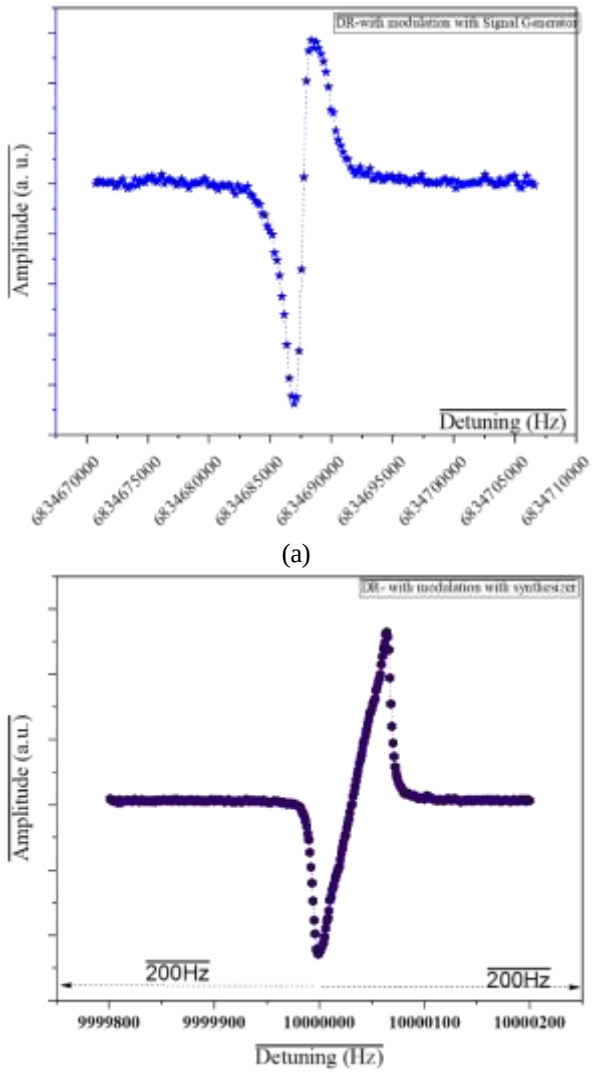


Fig. 2. (a) Double resonance spectrum obtained using the frequency modulation technique with a signal generator, featuring a central applied frequency of approximately 6.834 GHz, swept over a ±17.5 KHz range around the central frequency with an output power of 25 dBm.(b) Double resonance spectrum obtained using the frequency modulation technique with a frequency synthesizer, featuring a central applied frequency of approximately 10 MHz, swept over a ±200 Hz range around the central frequency with an output power of 25 dBm.

It is worth noting that the low modulation voltage is used to maintain the frequency deviation within the detection threshold. By adjusting the resistance value, the frequency deviation corresponding to the modulation frequency can be minimized, allowing the output to lock precisely onto a single target frequency. After incorporating the synthesizer in this configuration, the experimental setup is modified as illustrated in Fig. 1(b). The double-resonance data obtained using the synthesizer is presented. In Fig. 2(b), the frequency modulation (FM) data obtained by the synthesizer are shown. The dispersion-like profile observed in this spectrum corresponds precisely at its inflection point to the atomic clock transition, as indicated in Fig. 1(a). This behavior is consistent with the data shown in Fig. 2(a), confirming that the inflection point of the FM signal coincides with the atomic clock transition frequency.

III. CONCLUSION

By comparing the two data sets obtained above, we have effectively replaced a large and expensive signal generator system with a compact and low-cost frequency synthesizer. Upon examining Figs. 2(a) and 2(b), several important observations can be made. A key point is that in the case of the signal generator, a microwave frequency of approximately 6.834 GHz was applied, and a frequency sweep of about 35 kHz was required to locate the atomic transition.

However, in the case of the synthesizer, we applied a frequency of around 10 MHz with only a 400 Hz sweep, which clearly demonstrates the high precision and fine control of internal coefficients in the synthesizer system. And also, with greater and more stringent precision in Fig. 2(b) compared to Fig. 2(a), as mentioned above regarding the resistor and the capacitors, this slope is caused by the presence of the resistor and by the imprecise and non-optimal value of the applied resistor; removing the DC offset of the current will eliminate this slope.

REFERENCES

[1] C. Li, F. Sun, J. Liu, X. Li, D. Hou, and S. Zhang. "Continuous microwave-to-optical transduction with atomic beam fluorescence," Appl. Phys. Lett., pp. 154001(1-7), Vol. 119, 2021.

[2] M. Asadolahsalmanpour, M. Mosleh, and S.M. Hamidi. "Bloch surface wave-atom coupling in one-dimensional photonic crystal structure," Opt. Express, Vol. 31, pp. 4751-4759, 2023.

[3] M. Asadolahsalmanpour, M. Mosleh, and S.M. Hamidi. "Dual-frequency modulation in

[Downloaded from mail.ijop.ir on 2026-11-26]

microwave-optical double resonance for manipulation of atomic populations," Sci. Reports, Vol. 15, pp. 21264(1-6), 2025.

[4] H. Shi, J. Ma, X. Li, J. Liu, C. Li, and S. Zhang. "A Quantum-Based Microwave Magnetic Field Sensor," Sensors, Vol. 18, pp. 3288(1-14), 2018.

[5] A. Mirazei, M. Sotoudeh, M. Asadolah Salmanpour, S.M. Hamidi. "Tunable scheme of phase modulation in Rabi resonance in a natural rubidium vapor cell," Optik, Vol. 348, pp. 172690(1-10), 2026.

[6] F. Sun, Z. Jiang, J. Qu, Z. Song, J. Ma, D. Hou, and X. Liu. "Tunable microwave magnetic field detection based on Rabi resonance with a single cesium-rubidium hybrid vapor cell," Appl. Phys. Lett., Vol. 113, pp. 172690(1-6), 2018.

[7] F.Y. Sun, D. Hou, Q.S. Bai, and X.H. Huang. "Rabi resonance in Cs atoms and its application to microwave magnetic field measurement," J. Phys. Commun., Vol. 2, pp. 015008(1-10), 2018.

[8] F. Sun, J. Ma, Q. Bai, X. Huang, B. Gao, and D. Hou. "Measuring microwave cavity response using atomic Rabi resonances," Appl. Phys. Lett., Vol. 111, pp. 051103(1-6), 2017.

[9] A.B. Post, Y.Y. Jau, N.N. Kuzma, and W. Happer. "Amplitude-versus frequency-modulated pumping light for coherent population trapping resonances at high buffer-gas pressure," Phys. Rev. A—Atomic, Mol. Opt Phys, Vol. 72, pp. 033417(1-17), 2005.

[10] A. Mirzaei, M. Asadollahsalmanpour, M. Sotoudeh, M. Mosleh, and S.M. Hamidi. "High Signal to Noise Ratio in Miniaturized Atomic Cells by Frequency Modulation Spectroscopy Method," Pione. Adv. Mat , Vol. 1, pp. 1-7, 2026.

[11] A.S. Brannon, "Design and implementation of microwave VCOs for chip-scale atomic clocks," Disser. Abs. Inter. Vol. 68, pp. 1-212, 2007.

[12] X. Liu, Z. Jiang, J. Qu, D. Hou, X. Huang, and F. Sun. "Microwave magnetic field detection based on Cs vapor cell in free space," Rev. Sci. Instrum., Vol. 89, pp. 033417(1-7), 2018.

[13] J.G. Coffer, B. Sickmiller, A. Presser, and J.C. Camparo. "Line shapes of atomic-candle-type Rabi resonances," Phys. Rev. A, Vol. 66, pp. 023806(1-7), 2002.

[14] I. Eisele and L. Kevan. "Double modulation method for hall effect measurements on photoconducting materials," Rev. Sci. Instrum., Vol. 43, pp. 189-194, 1972.



Ali Mirzaei is working as a PhD student at the Laser and Plasma Research Institute in the Magnetoplasmonic Laboratory at Shahid Beheshti University, Tehran, Iran and is working on the Rabi resonance field, rubidium hot vapor and quantum clocks.



Danial Cheraghian received his MSc degree from Shahid Beheshti University, Tehran, Iran in 2025. Now he is working on electronic part of quantum sensors.



Mahnaz Asadolah Salmanpour received her PhD degree from Shahid Beheshti University in 2025. Now she is working on optical part of quantum sensors.

[Downloaded from mail.ijop.ir on 2026-11-26]



Mohammad Mosleh received his PhD in photonic from Shahid Beheshti University, Tehran, Iran. He is experienced in laser spectroscopy of alkali vapors, with applied expertise in quantum sensing. His research further includes studying novel miniaturization approaches, including surface wave- atom spectroscopy for chip-scale alkali vapor-based sensing applications. His current research concentrates on quantum computing with trapped ions, with the main goal of enhancing key system benchmarks such as fidelity, gate speed, qubit connectivity, and number of computational qubits.



Seyedeh Mehri Hamidi received her Ph.D. degree in photonics from the Laser and Plasma Research Institute, Shahid Beheshti University, Tehran, Iran, in 2009. She is currently the director of the Magneto-Plasmonic Lab of Laser and Plasma Research Institute. She works in the research fields of quantum photonics, atomic clocks, magneto-plasmonic, nanophotonic, neurophotonics, piezotronics, photonic and magnetophotonic crystals, surface plasmon resonance, dielectric, and magnetic nanostructures.

[Downloaded from mail.ijop.ir on 2026-11-26]

THIS PAGE IS INTENTIONALLY LEFT BLANK.

[Downloaded from mail.ijop.ir on 2026-11-26]